Electronic Supplementary Material (ESI) for Nanoscale Advances.

Hierarchical Hollow Porous Structures of Nickel Doped λ-MnO_2 Anode for Li-ion Energy Storage Systems

Venugopal Nulu, Arunakumari Nulu, Keun Yong Sohn*

Department of Nanoscience and Engineering, Center for Nano Manufacturing, Inje University, 197 Inje-ro, Gimhae, Gyeongnam-do 50834, Republic of Korea

* Correspondence to: K. Y. Sohn, Department of Nanoscience and Engineering, Center for Nano Manufacturing, Inje University, 197 Inje-ro, Gimhae, Gyeongnam-do 50834, Republic of Korea

E-mail addresses: ksohn@inje.ac.kr

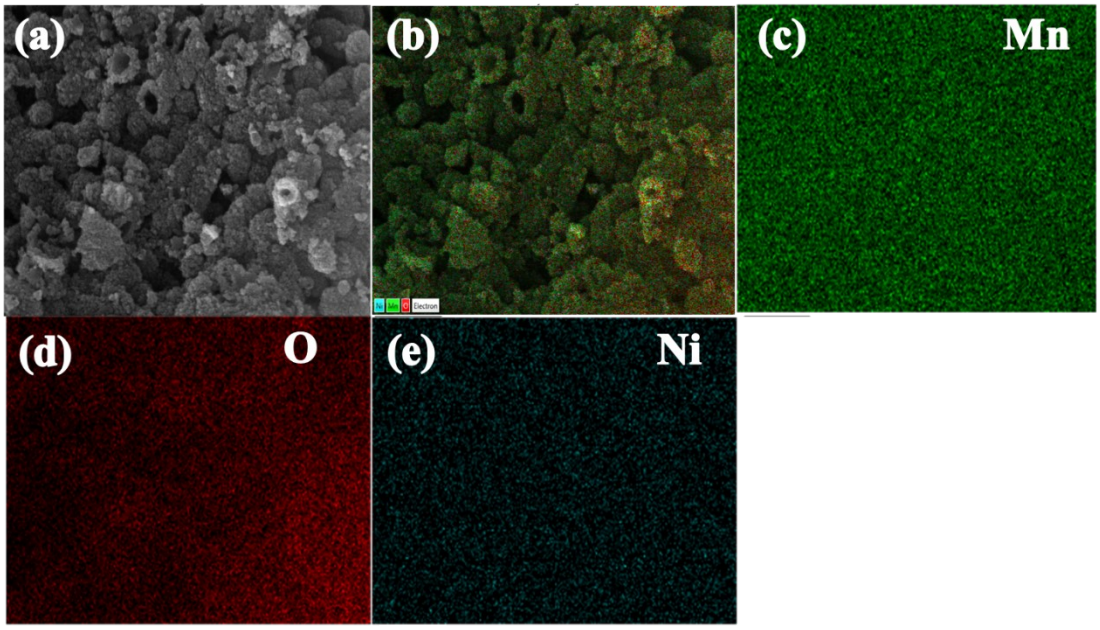

Figure S1. a) SEM image, b) SEM image comprised of layered elemental mappings containing Mn (image c), O (image d), and Ni (image e) of 20Ni-hMO.

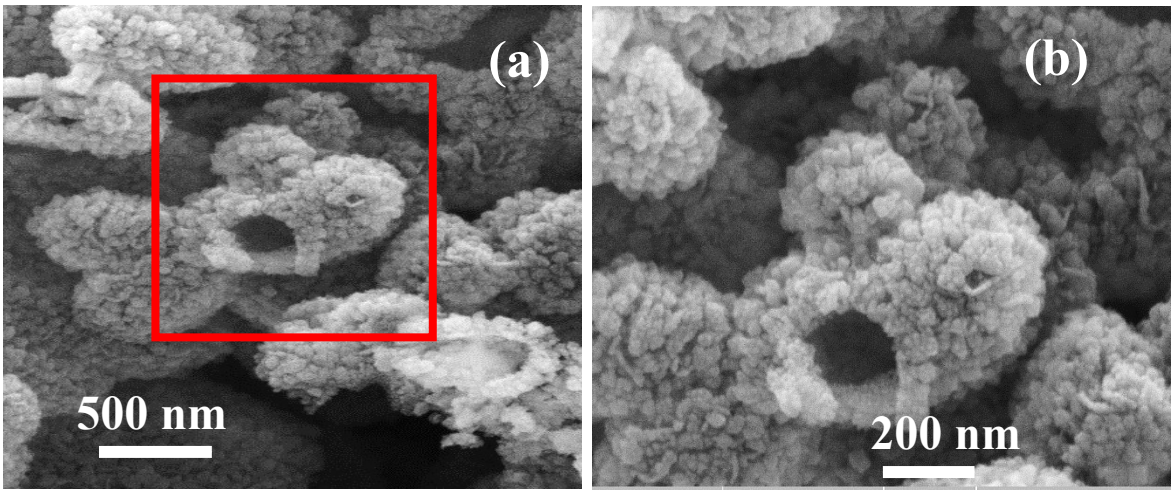

Figure S2. a) FE-SEM image of an aggregated group of h-MO three-dimensional hollow particles and b) is the close view of the selected hollow particle shown in the image (a).

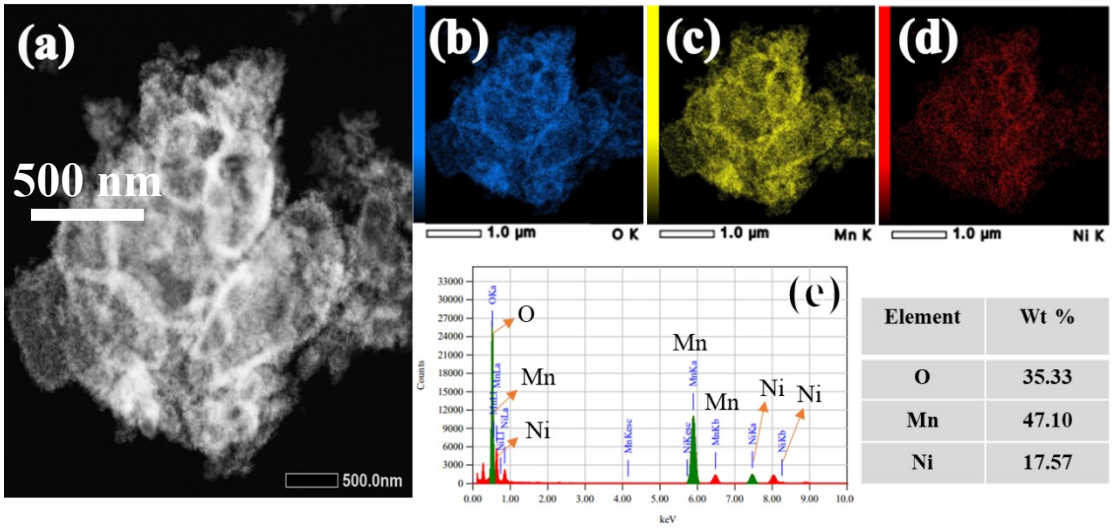

Element	Wt %
O	35.33
Mn	47.10
Ni	17.57

Figure S3. a) STEM image of 20Ni-hMO and the respective elemental mappings of (b) Mn (c) O (d) Ni, respectively. (e) TEM-EDX spectra with elemental composition table.

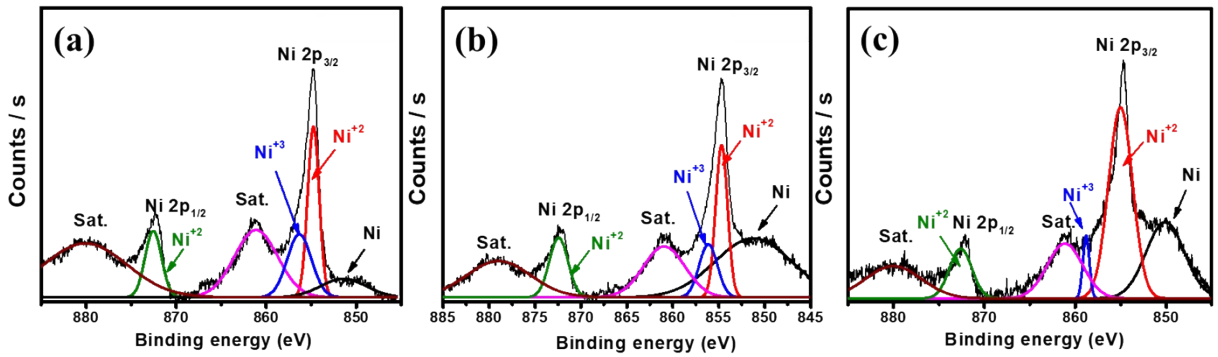

Figure S4. XPS spectra of Ni2p and Ni^0 for the three Ni doped samples. (a) 10Ni-hMO (b) 20Ni-hMO and (c) 30Ni-hMO.

Name	Peak BE	Atomic %	Mass %
Ni $2p^3$	852.37	7.30	15.9
Mn $2p^3$	640.12	29.58	51.4
O 1s	527.27	63.12	32.7

Table S1. Elemental surface atomic percentages of 20Ni-hMO sample obtained by XPS.

Sample	**Concentration (%)**		
	Ni	Li	Mn
λ-MnO_2 (h-MO)	-	2.10	76.30
20% Ni doped λ-MnO_2 (20Ni-hMO)	16.54	2.27	71.42

Table S2: The actual elemental compositions of h-MO and 20Ni-hMO samples from ICP-OES.

Name	Area under the curve(%)		
	Ni^{+2}	Ni^{+3}	Ni^{0}
10Ni-hMO	16.4	12.4	6.1
20Ni-hMO	14.4	7.8	33.8
30Ni-hMO	36.2	3.2	18.2

Table S3: Comparison of the percentages of Ni oxidation states in the three Ni-doped samples obtained by XPS.

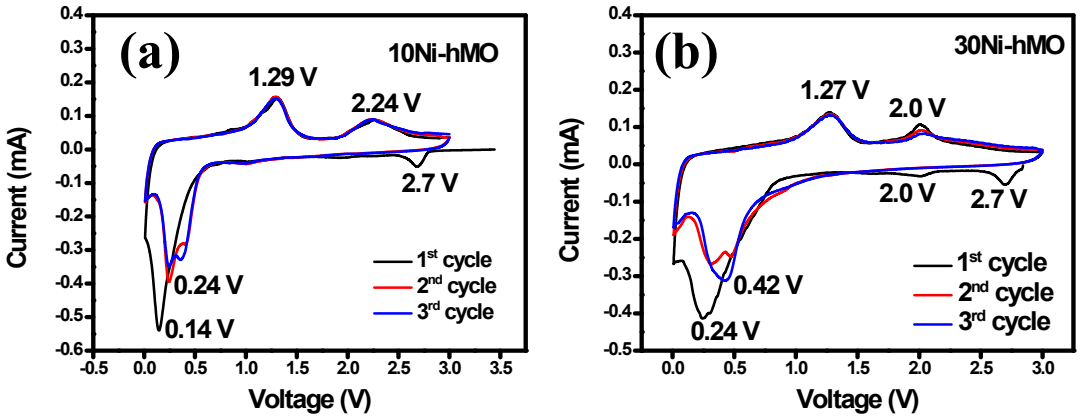

Figure S5. Cyclic voltammograms for the first three cycles of (a) 10Ni-hMO (b) 30Ni-hMO at a scan rate of 0.1 mV s^{-1}

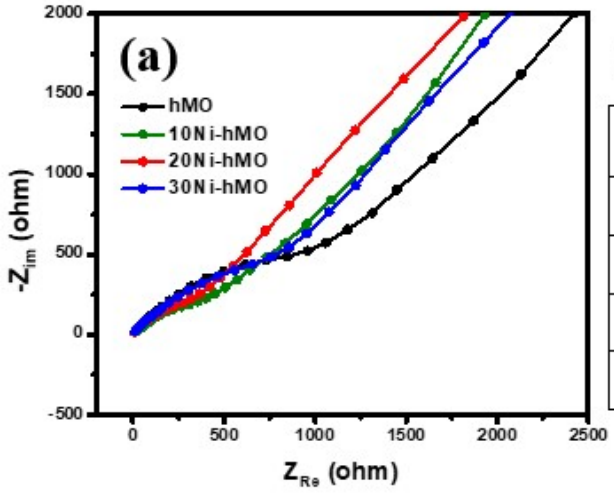

(b)

Electrode	R_s (Ω)	R_{ct} (Ω)
hMO	11.9	875.54
10Ni-hMO	13.3	502.25
20Ni-hMO	7.3	428.39
30Ni-hMO	10.9	727.24

Figure S6. Nyquist plots of the fresh h-MO, 10Ni-hMO, 20Ni-hMO, and 30Ni-hMO electrodes. (b) Tabulated parameter values for the electrodes.

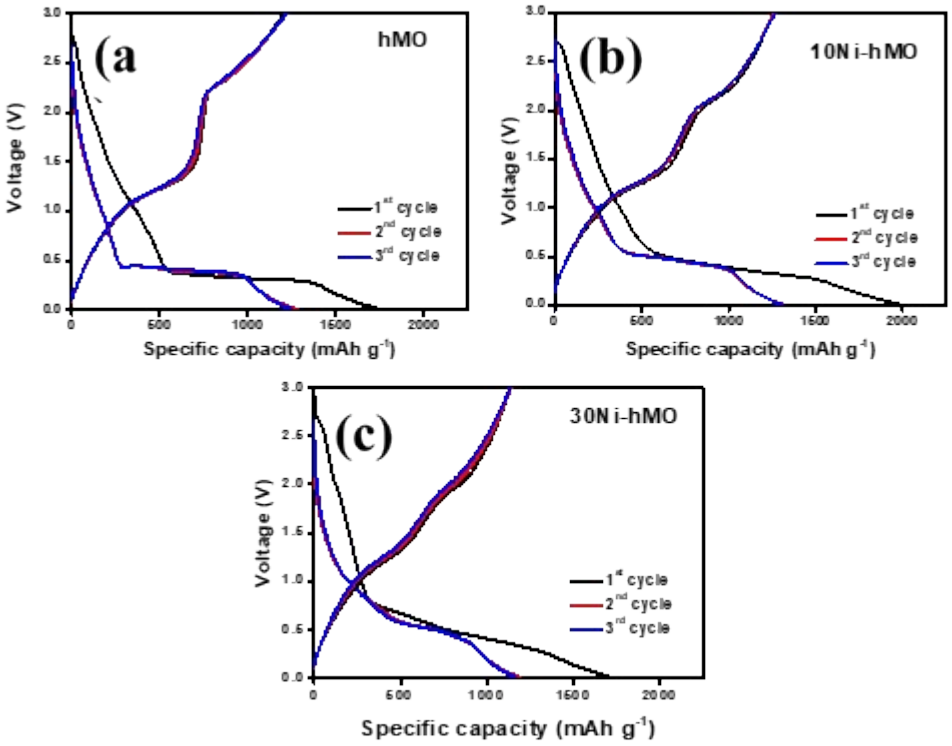

Figure S7. The respective charge–discharge profiles for the 1st, 2nd,and 3rd cycles of the h-MO and Ni-doped MnO_2 electrodes cycled at 200 mAh g^{-1} (see Fig. 8a in the main data) are shown in (a, b, c).

Electrode	R_s (Ω)	R_{SEI} (Ω)	R_{ct} (Ω)	D (cm^2s^{-1})
hMO	11.0	16.2	30.4	6.91×10^{-13}
10Ni-hMO	5.4	18.2	32.1	7.23×10^{-13}
20Ni-hMO	5.2	12.4	20.8	2.24×10^{-12}
30Ni-hMO	7.5	19.3	36.3	1.08×10^{-12}

Table. S4. Summarized circuit (shown in Fig. 9) parameters values.

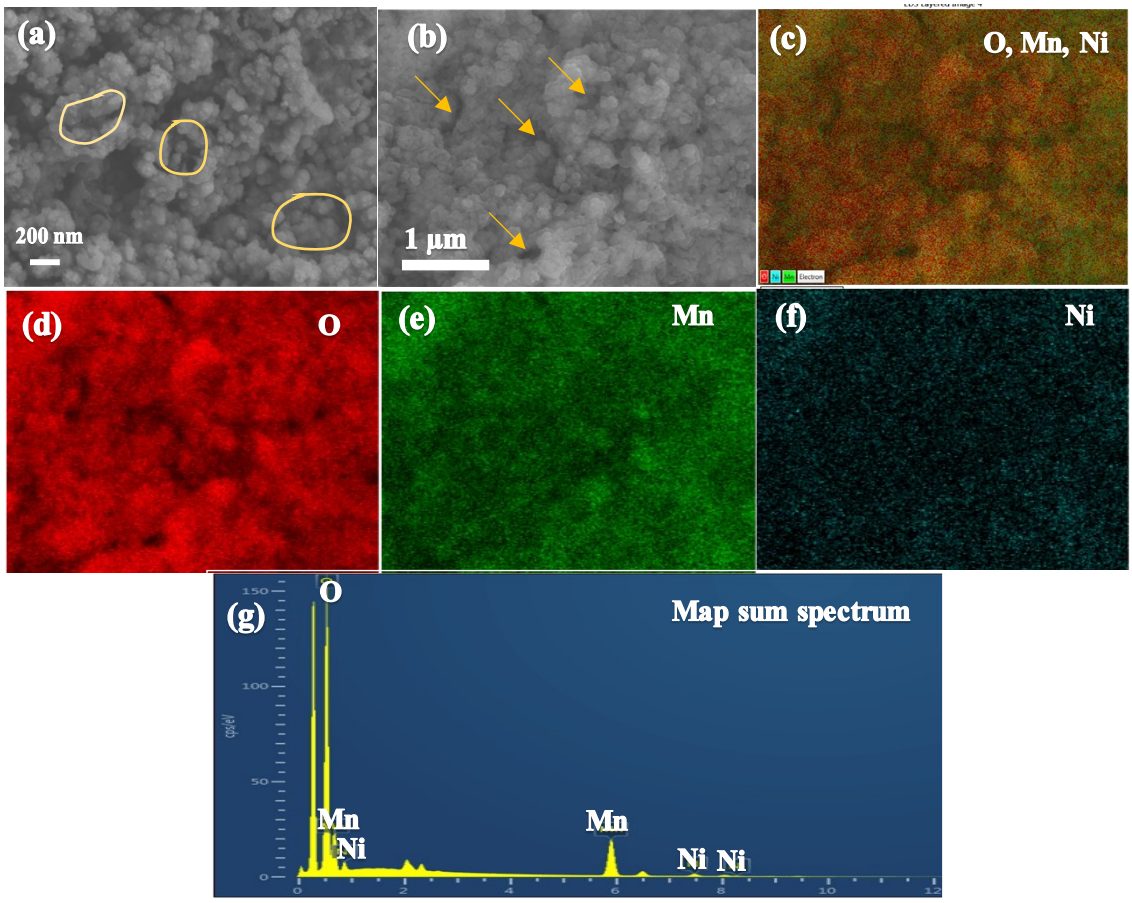

Figure S8. (a, b) SEM images of the anode 20Ni-hMO after cycling. (c) Layered mapping of the elements, elemental mapping of (d) O (e) Mn (f) Ni and (g) SEM-EDAX spectra of image (b).

Material	**Applied current**	**Initial coulombic efficiency(ICE)**	**Discharge capacity 2nd cycle**	**Discharge capacity (after cycling)**	**Ref.**
Nanotube	80 mA g^{-1}	25.1 %	~300 mAh g^{-1}	~110 mAh g^{-1} (40th cycle)	1
Microsphere	500 mA g^{-1}	61.3 %	~1000 mAh g^{-1}	~220 mAh g^{-1} (100th cycle)	2
Nanoparticle	100 mA g^{-1}	51.7 %	~630 mAh g^{-1}	~450 mAh g^{-1} (10th cycle)	3
Nanorod	100 mA g^{-1}	70.3 %	~1230 mAh g^{-1}	~1075 mAh g^{-1} (100th cycle)	4
Nanoflake	500 mA g^{-1}	33.8 %	~700 mAh g^{-1} (4th cycle)	~560 mAh g^{-1} (100th cycle)	5
Hollowcube	50 mA g^{-1}	27.2 %	~400 mAh g^{-1}	~281 mAh g^{-1} (500th cycle)	6
Nanowire	123 mA g^{-1}	31.7 %	~500 mAh g^{-1}	~250 mAh g^{-1} (100th cycle)	7
Ni-doped porous hollow MnO_2	200 mA g^{-1}	72.7%.	1429 mAh g^{-1}	1636 mAh g^{-1} (50th cycle)	This work

Table S5: Comparison between our Ni-doped MnO_2 (20Ni-hMO) hollow nanostructured anode material and the recently reported different nanostructures of MnO_2 and their carbon hybrid and Ni doped MnO_2 structures for LIBs.

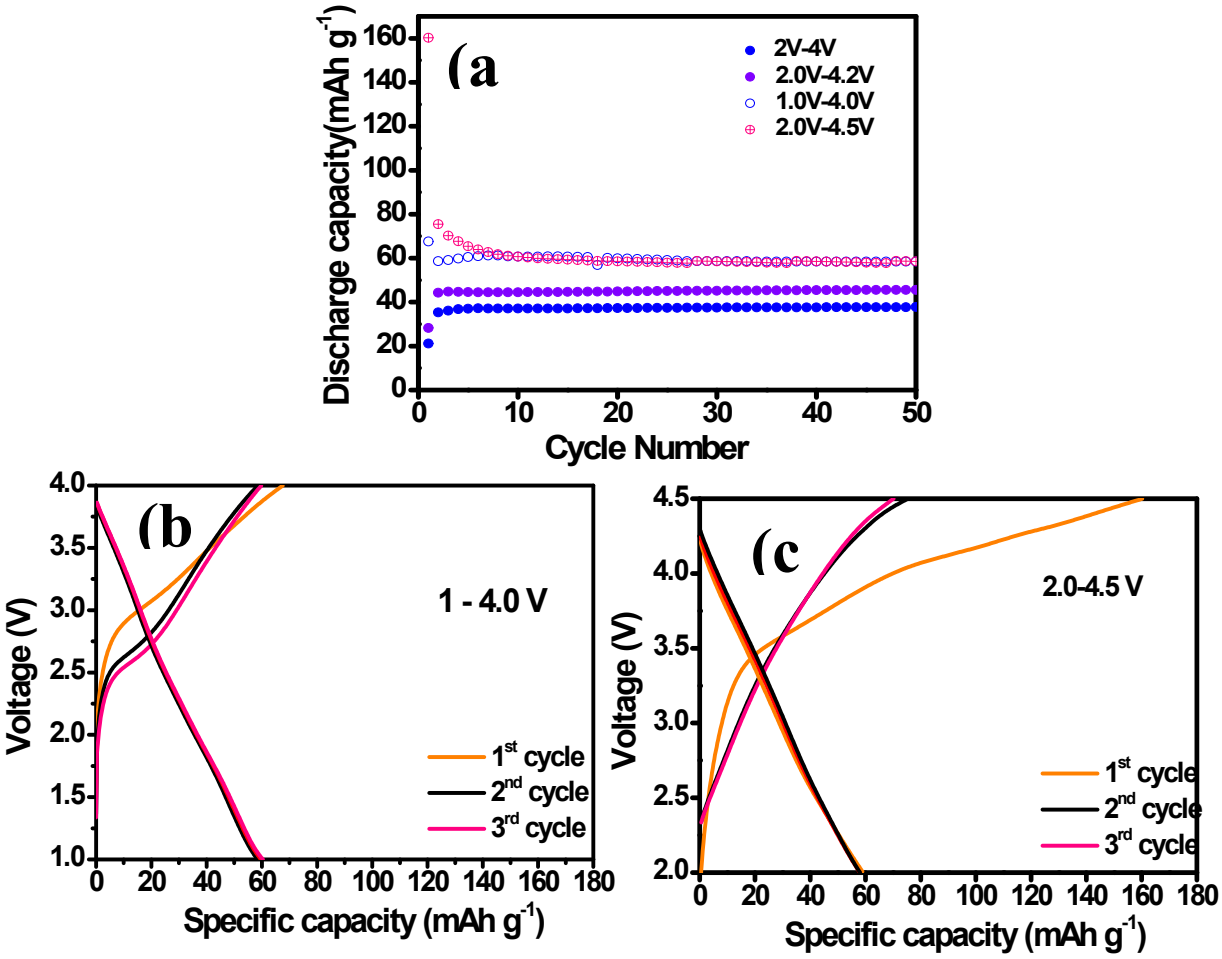

Figure S9. (a) Galvanostatic charge-discharge cycling performance of AC at different voltages at a current density of 100 mA g^{-1}. Charge-discharge curves of AC cycled between (b) 2-4.5 V (c) 1-4.0 V.

References

1. Y. S. Ding, X. F. Shen, S. Sithambaram, S. Gomez, R. Kumar, V. M. B. Crisostomo, S. L. Suib, M. Aindow, *Chem. Mater*. 2005, **17**, 5382.

2. Y. S. Horn, S. A. Hackney, C. S. Johnson, M. M. Thackeray, *J. Electrochem. Soc*. 1998, **145**, 582.

3. M. Toupin, T. Brousse, D. Bélanger, *Chem. Mater*. 2004, **16**, 3184.

4. L. Gao, L. Zhang, S. Jia, X. Liu, Y. Wang, S. Xing, *Electrochim. Acta*, 2016, **203**, 59.

5. H. Chen, B. Zhang, F. Li, M. Kuang, M. Huang, Y. Yang, Y. X. Zhang, *Electrochim. Acta*, 2016, **187**, 488.

6. R. N. Reddy, R. G. Reddy, *J. Power Sources*, 2004, **132**, 315.

7. J. Cao, Q. Mao, L. Shi, Y. Qian, *J. Mater. Chem*. 2011, **21**, 16210.